Advanced Study of Switchable Spin Crossover Compounds

Gavin Craig

ADVANCED STUDY OF SWITCHABLE SPIN CROSSOVER COMPOUNDS

Universitat de Barcelona

Facultat de Química

Departament de Química Inorgànica

Programa de Doctorat: Química Inorgànica Molecular

Grup de Magnetisme i Molècules Funcionals

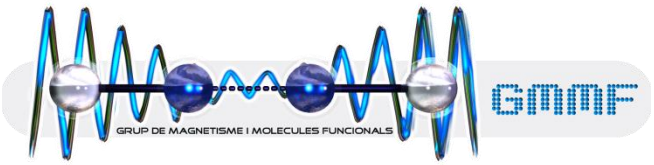

Gavin Craig

Director: Dr. Guillem Aromí Bedmar, Departament de Química Inorgànica

Tutor: Dr. Santiago Alvarez Reverter, Departament de Química Inorgànica

Contents

Chapter 8: Mononuclear Fe(II) compounds containing the ligand 2,6-Bis(5-(2-methoxyphenyl)-pyrazol-3-yl)pyridine

8.0 Introduction

As highlighted by Goodwin, a proposed strategy for the modulation of the cooperativity in SCO compounds is to vary the hydrogen bonding moieties present in the crystal lattice.[1] It follows that the magnetic properties can be toggled by changing these donors. Most commonly, as demonstrated in Chapters 6 and 7, this is achieved by varying the anion and solvent content of the sample. However, another method would be to change the functionality of the ligand.[2-5]

One example of this approach is the series of Fe(II) compounds based on $[Fe(bapbpy)(NCS)_2]$ (bapbpy = N6,N6'-di(pyridine-2-yl)-2,2'-bipyridine-6,6'-diamine). The original compound was found to display a two-step SCO, with hysteresis loops associated to each transition.[6, 7] The system's SCO behaviour was found to be particularly rich, with the transition also brought about by the application of pressure, and dependent on the sample preparation.[8-10] A further work modified the ligand, replacing the terminal pyridyl rings with picoline or quinoline groups.[11] The results were varied, ranging from a one-step SCO with hysteresis, through to the complete removal of spin transition.

Therefore, the ligand modification strategy has been used here, by synthesising H_2L1, which contains a methoxyphenyl ring rather than the hydroxyphenyl ring of H_4L (Scheme 8.1). This affords two important changes compared to H_4L: firstly, the distal methoxy group's steric bulk group is greater than that of a hydroxyl- group, impacting on the supramolecular chemistry of the cations; and secondly, the absence of a proton on the oxygen atom should render the species inert to the fluoroboration process observed in H_4L in compound **8**. Thus, this ligand has been used to obtain several mononuclear Fe(II) compounds, whose structural and magnetic properties will be described in this Chapter.

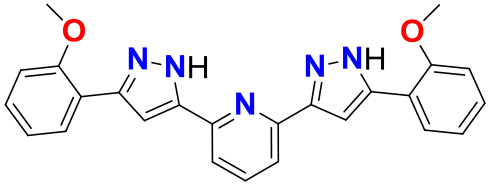

H_2L1

Scheme 8.1: 2,6-bis(5-(2-methoxyphenyl)-pyrazol-3-yl)pyridine (H_2L1)

8.1 Synthesis

The compounds described in this Chapter were obtained by reacting two molar equivalents of the ligand H_2L1 with one molar equivalent of a given Fe(II) salt, in the presence of ascorbic acid. The reaction and crystallisation conditions are summarised in Table 8.1. The majority of the complexes were obtained in the crystal form by layering the mother liquor of the reaction with a precipitating solvent, with hexane or diethyl ether being the most effective solvents for this purpose. One of the motivations for the development of the ligand H_2L1 was to prevent the possible fluoroboration[12] of the ligand on coordination to Fe(II) in the presence of tetrafluoroborate, which occurred in compound **8**. This strategy was successful in the syntheses of compounds **12** and **13**, which contain both the intact polypyrazolyl ligand and two BF_4^- anions to compensate for the charge of the metal centre, demonstrated by single crystal X-ray diffraction studies (Section 8.2). Although compound **15** has been obtained as crystals, the crystal structure has not, as yet, been obtained, although a composition is suggested on the basis of EA, and the magnetic properties presented. In the case of compound **14**, there is disordered solvent molecule which couldn't be definitively identified. As yet, a bulk magnetic measurement has not been carried out, and the description here is limited to the observation of the deformation around the coordination sphere in the crystal structure, which allows a prediction of the magnetic behaviour.

Compound	Ligand	Anion	Reaction Solvent	Crystallisation
11		ClO_4^-	Acetone	Layer, Hexane
12		BF_4^-	Acetone	Layer, Hexane
13	H_2L1	BF_4^-	Ethanol	Slow evaporation
14		$CF_3SO_3^-$	Propan-2-ol	Layer, Ether
15		$CF_3SO_3^-$	Acetone	Layer, Hexane

Table 8.1: Reaction conditions for the compounds described in Chapter 8.

8.2 Single crystal X-ray diffraction study

The compounds **11**, **12**, **13**, and **14**, are structurally related, in that they all contain an $[Fe(H_2L1)_2]^{2+}$ cation, which consists of two molecules of the ligand H_2L1 chelating to an Fe(II) centre through the central nitrogen atoms. The cell content is then determined by the solvent employed in the reaction, and the conditions used to obtain crystals. The

Compound	11	12	13	14
T/K	100(2)			
crystal system	Monoclinic	Triclinic	Triclinic	Monoclinic
space group	$P2_1/c$	P-1	P-1	$P2_1/c$
a/Å	12.546(1)	11.937(3)	11.983(1)	12.449(2)
b/Å	18.797(2)	12.089(3)	13.069(1)	19.087(2)
c/Å	24.113(3)	20.856(6)	18.665(4)	25.100(3)
α/°	90	85.262(10)	87.836(2)	90
β/°	97.604(2)	79.723(12)	79.826(2)	95.320(2)
γ/°	90	89.013(9)	76.103(2)	90
V/Å^3	5635.9(11)	2951.2(13)	2793.1(6)	5938.4(13)
μ/mm^{-1}	0.431	0.345	0.357	0.517
reflections collected	7074	10411	10936	12113
R1 (all data)	0.1105	0.0847	0.1192	0.0858
wR2 (all)	0.3678	0.2314	0.2831	0.2771
S	1.62	1.09	1.19	1.10
av. Fe-N/Å	2.176	2.174	2.186	2.171
octahedral volume/Å^3	12.033	11.866	12.123	11.982
Σ/°	158.79	167.44	169.35	161.77
Φ/°	153.47	154.04	153.33	155.53
θ/°	89.86	76.64	79.35	86.05
Θ/°	492.23	507.06	491.20	499.81

Table 8.2: Crystallographic data and selected distortion parameter for compounds **11**-**14**.

average Fe-N bond lengths range from 2.171-2.186 Å, which indicates that at 100 K, all four systems are in the HS state (Table 8.2).[13] Figure 8.1 shows the cation in compound **11**, with the table displaying the six Fe-N bond lengths. Compound **11** crystallises in the monoclinic space group $P2_1/c$, and the asymmetric unit consists of one $[Fe(H_2L1)_2]^{2+}$ cation and one molecule of acetone. While all of the previously described systems with H_4L displayed one ligand with a *syn,anti* conformation and one with a *syn,syn* conformation of the phenol groups with respect to the central coordination pocket, in this compound the methoxyphenyl wings of the ligand are disordered. In one ligand, only one

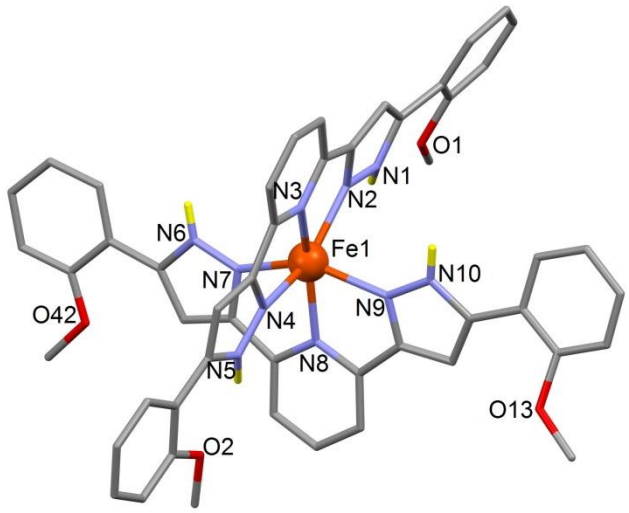

Bond	Bond length/Å
Fe-N3	2.142(6)
Fe-N8	2.141(5)
Fe-N2	2.173(5)
Fe-N4	2.234(5)
Fe-N7	2.170(5)
Fe-N9	2.195(5)
Average	2.176

Figure 8.1 and Table 8.3: A view of the $[Fe(H_2L1)_2]^{2+}$ cation in **11**; hydrogen atoms omitted for clarity, except those bonded to heteroatoms, shown in yellow. The six Fe-N bond distances are given in the table.

of the rings is disordered over two positions equally with the other ring featuring the *syn* conformation. In the other ligand, both rings are disordered equally over two positions. As a result, there are eight equally possible conformations of the $[Fe(H_2L1)_2]^{2+}$ cations (see Scheme 8.2). For the sake of brevity, only one of the combinations is described, the *syn*,*syn*,*anti*,*anti* conformation. The cation in **11** shows a large deviation of the parameter Φ from 180°,[14] measuring 153.47°. In fact, this large distortion of Φ is common to the

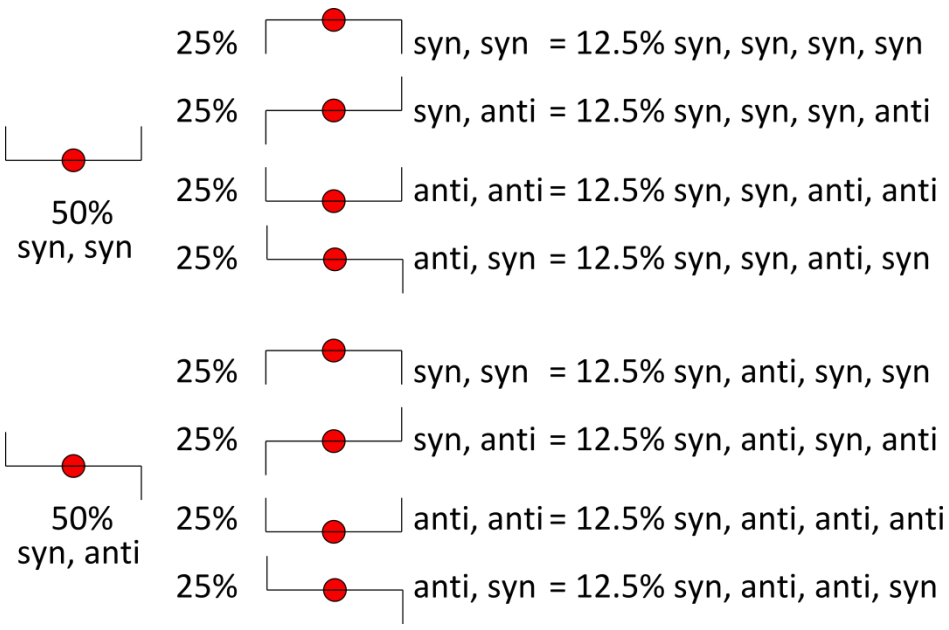

Scheme 8.2: Schematic representation of the different possible combinations of ligand disorder in the $[Fe(H_2L1)_2]^{2+}$ cations of **11**.

four systems, which collectively display an average value of 154.09°. Such deformation around the Fe(II) centre had previously been encountered in the compounds **4** and **5**, and those compounds together with those described in this Chapter constitute the most distorted systems in the family of 3-bpp derivatives (see Chapter 9).

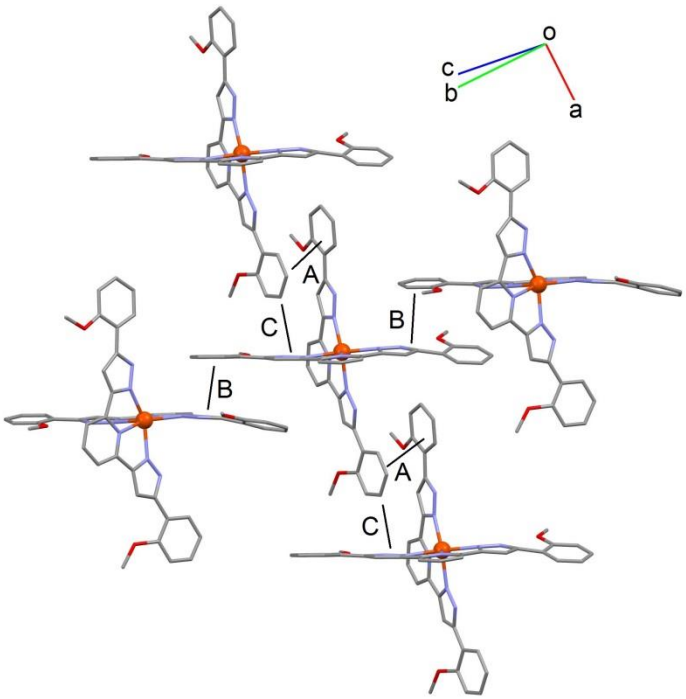

Contact	Labels	Distance/Å
π*···*π		
A	pz···phen	3.878(4)
B	pz···phen	4.246(5)
C-H···*π*		
C	C48-H48···pz	3.486(8)

Figure 8.2 and Table 8.4: The interactions involved in the assembly of the terpy embrace in **11**, with hydrogen atoms omitted for clarity.

The terpyridine embrace[15, 16] is present in compound **11**, although it contains fewer C-H···π contacts than in the full form of the packing motif. There do exist overlaps between the extended wings of the H_2L1 ligand, which is the basis of the co-planar arrays that form, however the contact is non-optimal, due to the planes of the participating aromatic rings not being parallel (Figure 8.2). Therefore, while the arrays may be observed, the packing is not as efficient as seen in other compounds presented in thesis. The deviation

of the angle Φ from 180° is notable in the layers, and the consequent displacement of the pyridyl rings prevents the face-to-face interactions between the layers.

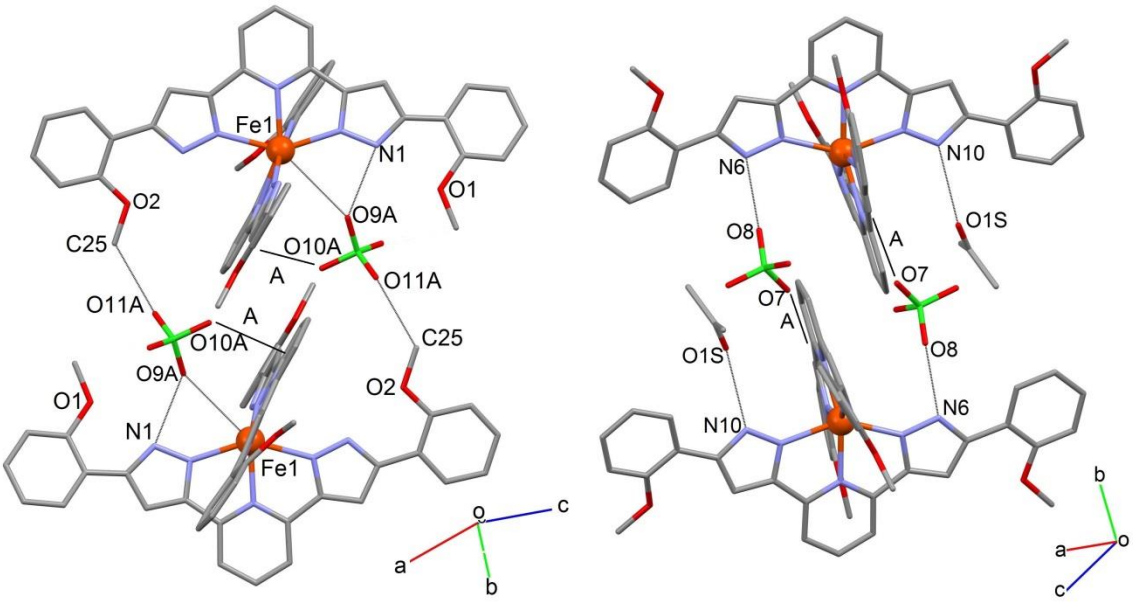

Contact	Distance/Å	Contact	Distance/Å
N1-H1···O9A	2.691(15)	**N6-H6···O8**	2.814(10)
O9A···Fe	3.277(3)	**N10-H10···O1S**	2.856(16)
C25-H25A····O11A	3.157(17)	**O7···H20-C20**	3.255(11)
O10A···py	2.961(11)		
Fe···Fe	10.171(3)	**Fe···Fe**	10.516(3)

Figure 8.3 and Table 8.5: The hydrogen bonding motifs and metric parameters for the interactions that exist between the 2D layers in **11**, with hydrogen atoms omitted for clarity.

This deviation in the value of Φ, as analogously described in Chapter 6, has the effect of closing off one of the pyrazolyl rings of a coordinated H_2L1 ligand, preventing its participation in intermolecular contacts (Figure 8.3). However, in **11**, the steric bulk of the methoxy group forces the perchlorate anion further in towards the core of the cation. Consequently, the perchlorate anion not only forms a hydrogen bond with the pyrazolyl ring of the ligand, but also dispays a contact with the Fe(II) centre (O9A···Fe1 = 3.277(3) Å). This anion also partakes in an anion···π contact[17, 18] with the pyridyl ring of an H_2L1 ligand, and bridges to the adjacent cation through a weak O···H-C interaction. In the other possible set of interactions that link adjacent cations, both pyrazolyl rings form hydrogen bonds – one to a solvent molecule of acetone, the other to a perchlorate anion.

This perchlorate then bridges to the adjacent cation through a weak O···H-C contact with the edge of the aromatic rings, while the acetone molecule participates in H···H contacts with other entities in the lattice.

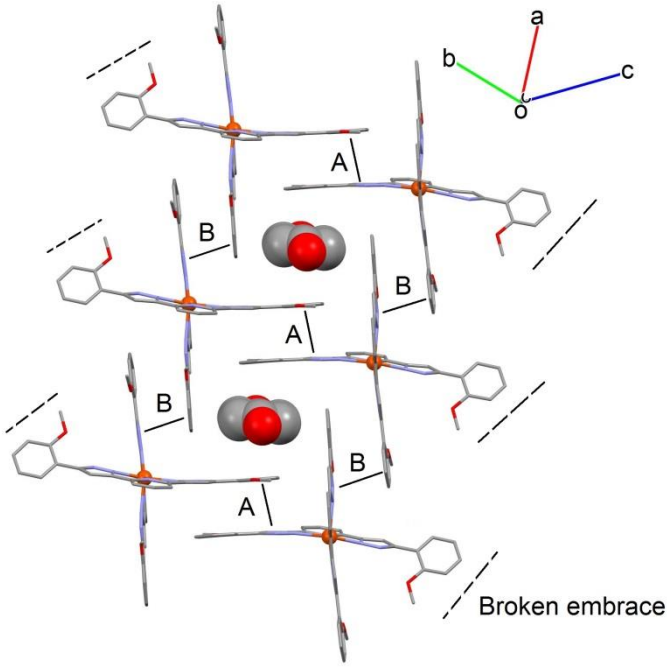

Contact	Labels	Distance/Å
π···π		
A	pz···phen	3.677(3)
B	pz···phen	3.752(3)

Figure 8.4 and Table 8.6: The broken terpyridine embrace in compound **12** with the distances of the contacts given in the table.

Compound **12** crystallises in the triclinic space group P_{-1}, with one $[Fe(H_2L1)_2]^{2+}$ cation in the asymmetric unit, two tetrafluoroborate anions to balance the charge, three molecules of acetone, and a molecule of water. The nature of the crystal packing in this compound is decided by two different distortions, one in the wings of the ligand, and another around the Fe(II) ions. The former concerns one of the methoxyphenyl rings that is found in the extremities of the cation which shows an unusally large degree of twisting out of the plane of the ligand. While these rings normally lie approximately within the plane of the central 3-bpp moiety, with a small inclination outwith that plane, **12** has an external ring which forms an angle of 52.6° between the plane of the methoxyphenyl ring and the plane of the 3-bpp core. The ramification of this twist is that within the co-planar

arrays of cations, the $\pi\cdots\pi$ interaction of one of the molecule's branches is prevented, interrupting the possible terpyridine embrace (Figure 8.4). This ring actually participates as the π-donor in a C-H$\cdots\pi$ interaction between the layers of cations (Figure 8.5).

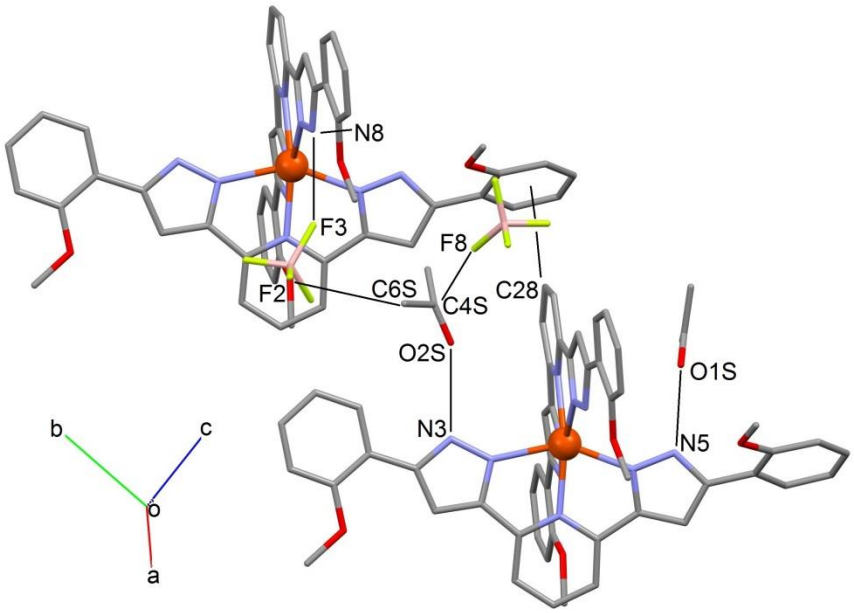

Contact	Distance/Å
N3-H3···O2S	2.851(6)
N5-H5···O1S	2.762(8)
N8-H8···F3	2.834(5)
F4···H6S1-C6S	3.551(4)
F8···C4S	2.925(5)
C28-H28A···phen	3.565(7)
Fe···Fe	12.089(4)

Figure 8.5 and Table 8.7: The hydrogen bonding motifs and metric parameters for the interactions that exist between the 2D layers in **12**, with hydrogen atoms omitted for clarity.

In the second distortion, measured by the angle Φ, one of the H_2L ligands blocks off a pyrazolyl ring (that of N10), in a manner similar to that seen in **11** (Figure 8.6). Consequently, only one of the pyrazolyl rings is available to participate in hydrogen bonding, and does so with a tetrafluoroborate anion. In the compounds containing the ligand H_4L, the adjacent cation would then have a hydroxyl group available to complete the bridge between the cations. Here, however, the methoxy group is sterically bulky, and so the anion interacts with the edge of the pyridyl ring of the adjacent cation. This causes

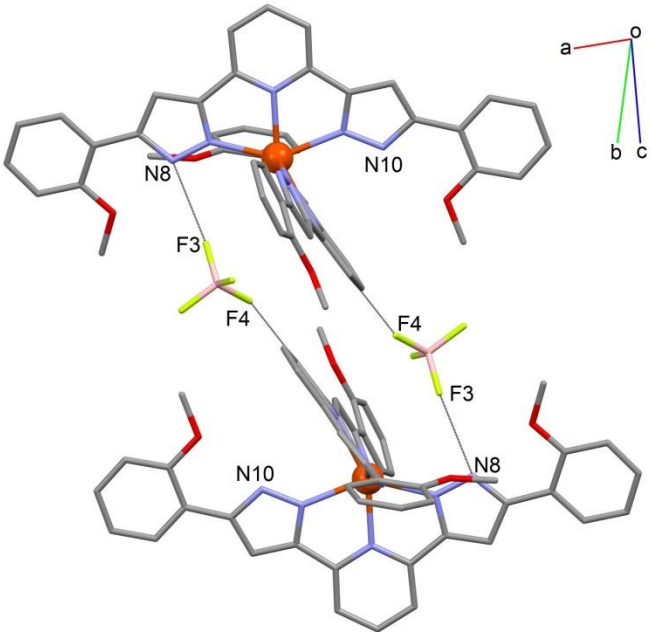

Contact	Distance/Å
N8-H8···F3	2.834(6)
F4···H2A-C2	3.434(7)
Fe···Fe	10.571(4)

Figure 8.6 and Table 8.8: The hydrogen bonding motifs and metric parameters for the interactions that exist between the 2D layers in **12**, with hydrogen atoms omitted for clarity.

a displacement of on cation with respect to the other, and the face-to-face pyridyl interactions seen in other compounds are prevented.

Compound **13** also crystallises in the triclinic space group $P\bar{1}$, and the unit cell contains two $[Fe(H_2L1)_2]^{2+}$ cations, balanced in charge by four tetrafluoroborate anions, and complemented by five lattice molecules of ethanol. As in **11**, there is disorder of the coordinated ligands, although in this case it is to a lesser extent. Here, just one ligand has

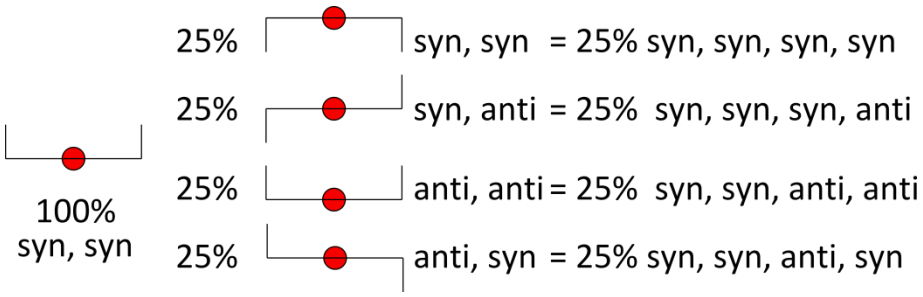

Scheme 8.3: Schematic representation of the different possible combinations of ligand disorder in the $[Fe(H_2L1)_2]^{2+}$ cations of **13**.

both methoxyphenyl rings disordered, both over two positions of equal occupancy. Therefore, there are four possible conformations of the cations (Scheme 8.3). Only the case for *syn,syn,syn,anti* will be described. The deformation of the angle Φ is sufficiently strong to close off one pyrazolyl ring, and the tetrafluoroborate anion is close enough to the Fe(II) centre to display an interaction with the metal. The mutual displacement of the cations that this imposes results in a lack of face-to-face interactions between the pyridyl

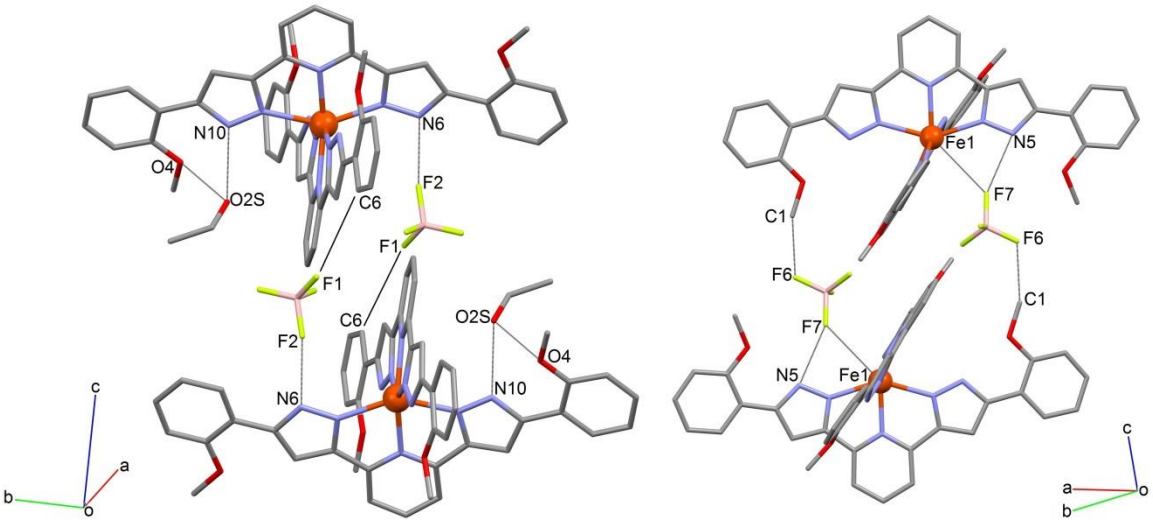

Contact	Distance/Å	Contact	Distance/Å
O4···O2S	2.251(8)	**N5-H5···F7**	2.696(11)
N10-H10···O2S	2.773(12)	**F6···H1A···C1**	3.093(6)
N6-H6···F2	2.755(7)	**F7···Fe1**	3.211(10)
F1···H6A···C6	3.381(9)		
Fe···Fe	10.683(3)	**Fe···Fe**	10.391(4)

Figure 8.7 and Table 8.9: The hydrogen bonding motifs and metric parameters for the interactions that exist between the 2D layers in **13**, with hydrogen atoms omitted for clarity.

rings that lie in the co-planar arrays of cations (Figure 8.7), which are formed by the terpyridine embrace. Instead, the bridge between cations in adjacent layers is made by the tetrafluoroborate anions, which participate in contacts between the pyrazolyl rings with the edge of the aromatic rings in the contiguous cations.

The aforementioned co-planar array of cations that are brought together in the terpyridine embrace in **13** are to be found in quite a regular arrangement (Figure 8.8). The conventional overlaps between the extended branches of the H_2L1 ligand are reinforced by two C-H$\cdots\pi$ interactions. Therefore, despite the presence of ethanol molecules in the

structure, the most important effect seen in the packing is the action of the tetrafluoroborate anions in conjunction with the steric bulk of the distal methoxyphenyl groups.

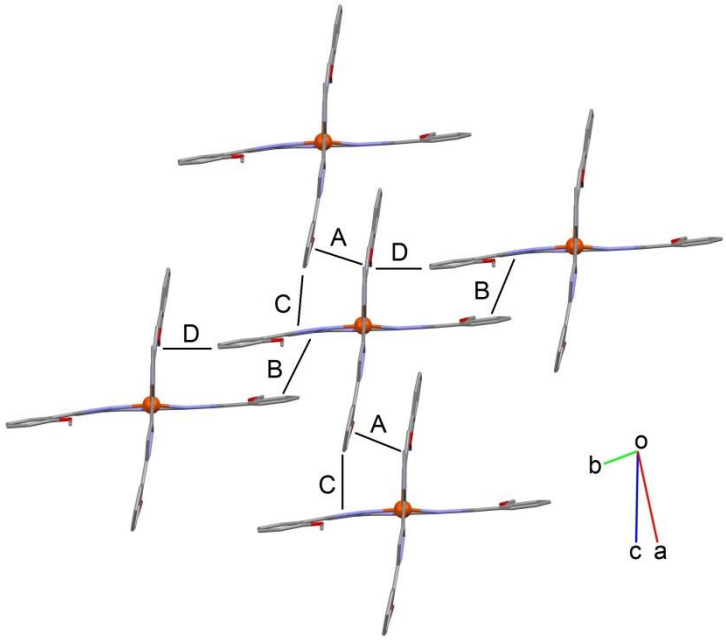

Contact	Labels	Distance/Å
π···π		
A	pz···phen	3.662(5)
B	pz···phen	4.189(5)
C-H···*π*		
C	C22-H22A···pz	3.718(6)
D	C47-H47A···pz	3.644(9)

Figure 8.8 and Table 8.10: A representation of the co-planar cations in **13**, induced by $\pi\cdots\pi$ and C-H$\cdots\pi$ interactions. Hydrogen atoms are omitted for clarity. The table details the distances for each contact at 100 K.

The crystal structure of compound **14** also displays disorder in the methoxyphenyl groups of the cation, although only in one ring of one H_2L1 ligand, leading to two possible overall conformations: *syn*,*anti*,*anti*,*syn*; and *syn*,*anti*,*anti*,*anti*. The description below involves the *syn*,*anti*,*anti*,*anti* configuration. The value of Φ of 155.53°, far from the ideal value of 180°, has the same effect as that seen in other compounds with similar distortions; one of the extended polypyrazolyl ligands leans towards the wing of another, closing off a pyrazolyl ring, and preventing it from participating in hydrogen bonding

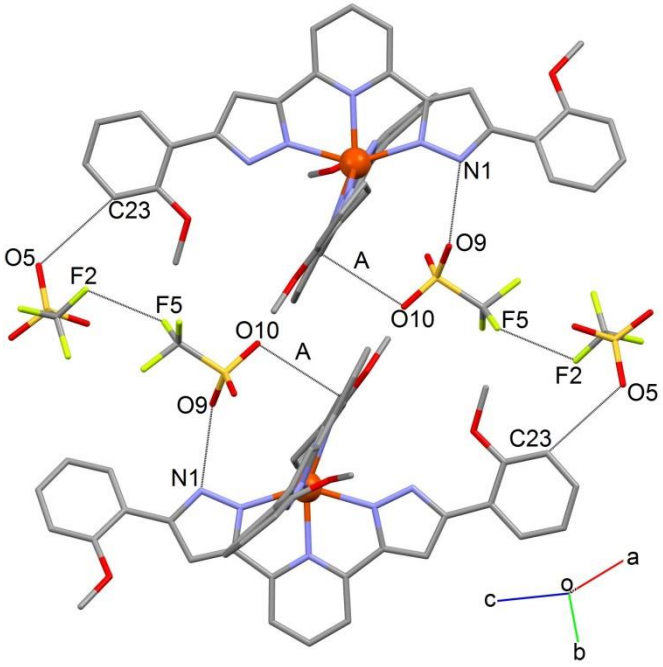

Contact	Distance/Å
N1-H1···O9	2.781(7)
F2···F5	2.801(12)
O5···H23A-C23	3.208(7)
A = O10···py	3.320(8)
Fe···Fe	10.658(1)

Figure 8.9 and Table 8.11: The hydrogen bonding motifs and metric parameters for the interactions that exist between the 2D layers in **14**, with hydrogen atoms omitted for clarity.

(Figure 8.9). The other pyrazolyl ring bridges to a triflate anion that also establishes an anion···π contact with the pyridyl ring of the adjacent H_2L1 ligand. This induces a mutual displacement of the pyridyl rings on neighbouring cations, and prohibits the formation of face-to-face contact between the two. The triflate anion responsible for this packing displays a contact with the other anion present in the lattice, which in turn links to the adjacent cation. Although a bulk measurement of the magnetic properties could not be carried out for this compound, the deformation around the Fe(II) cation, and the crystal packing observed has resulted in HS behaviour for other similar compounds, with an absence of SCO.

8.3 Magnetic properties

Magnetic susceptibility measurements were carried out on both single crystal samples and powder samples of compounds **11**, **12**, **13**, and **15** in the temperature range 5-300 K under an applied field of 5 kG (Figure 8.10, only the powder measurements shown). At 300 K, the compounds show values of χT of 3.70 (**11**), 3.53 (**12**), 3.74 (**13**), and 3.46 (**15**), due to Fe(II) ions in the HS state (χT = 3 $cm^3mol^{-1}K$ for S = 2, supposing g = 2.0).[19] On lowering the temperature at 1 $Kmin^{-1}$, the magnetic response for the compounds remains almost constant, until around 50 K, where the values of χT start to decrease due to zero field splitting effects,[20] giving χT = 2.93, 2.18, 2.06, and 2.89 $cm^3mol^{-1}K$ for **11**, **12**, **13**, and **15**, respectively, at the lowest temperatures measured. These data are consistent with four systems that remain in the HS state over the temperature range measured, and with the single crystal structures as resolved via diffraction studies.

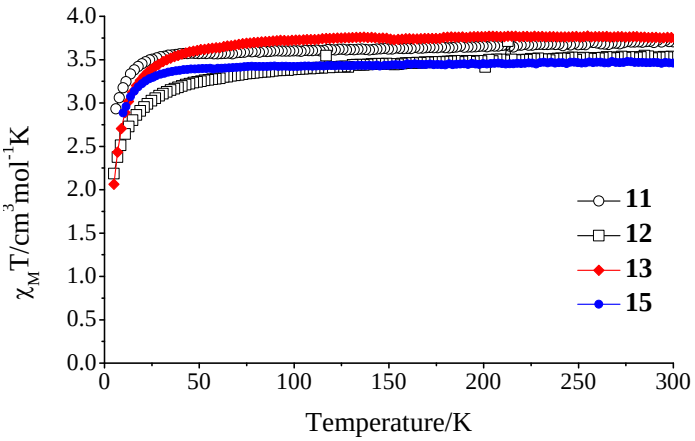

Figure 8.10: The molar magnetic susceptibility product, χT *vs*. the temperature, *T*, for the compounds described in this Chapter, in the temperature range 300 to 5 K , measured at a rate of 1 $Kmin^{-1}$.

8.4 Concluding remarks

The novel polypyrazolyl ligand H_2L1 has been used successfully to synthesise mononuclear Fe(II) compounds. The rationale behind the development of the ligand was to prevent the possible fluoroboration of the ligand on reaction with tetrafluoroborate salts (as observed in compound **8**), and this strategy proved to be effective in the synthesis of compounds **12** and **13**. Due to the steric bulk of the distal methoxy group, the charge-balancing anions are often pushed closer towards the centre of the cations, resulting in high distortions in the angle Φ. Extreme deviations of this parameter usually result in an

absence of SCO behaviour,[21] and this has been found to be the case in all of the systems studied here. In contrast to the case of the compounds containing H_4L, the majority of the compounds presented here display disorder of the methoxyphenyl rings of the ligand over two positions. This is attributed to the relatively weak intermolecular interactions in which this group participates. It could be suggested that the stronger hydrogen bonding group –OH, in H_4L, leads to stronger intermolecular contacts, and results in a more fixed organisation of the compounds within the crystal lattice. This "lability of interaction" of H_2L1 could be behind the absorption/desorption phenomena observed in another set of compounds currently being investigated in the group.[22] There, the release of solvent molecules from the solvent lattice is associated with a twist and re-alignment of the methoxyphenyl rings, which presumably wouldn't be possible were the interactions surrounding the ligand's wings of a stronger nature.

8.5 References

1. P. Gütlich and H. A. Goodwin, *Top. Curr. Chem.*, 2004, **233**, 1-47.
2. T. M. Pfaffeneder, S. Thallmair, W. Bauer and B. Weber, *New J. Chem.*, 2011, **35**, 691-700.
3. H. Petzold and S. Heider, *Eur. J. Inorg. Chem.*, 2011, 1249-1254.
4. R. González-Prieto, B. Fleury, F. Schramm, G. Zoppellaro, R. Chandrasekar, O. Fuhr, S. Lebedkin, M. Kappes and M. Ruben, *Dalton Trans.*, 2011, **40**, 7564-7570.
5. C. Carbonera, J. S. Costa, V. A. Money, J. Elhaik, J. A. K. Howard, M. A. Halcrow and J. F. Létard, *Dalton Trans.*, 2006, 3058-3066.
6. S. Bonnet, M. A. Siegler, J. S. Costa, G. Molnár, A. Bousseksou, A. L. Spek, P. Gamez and J. Reedijk, *Chem. Commun.*, 2008, 5619-5621.
7. S. Bedoui, G. Molnar, S. Bonnet, C. Quintero, H. J. Shepherd, W. Nicolazzi, L. Salmon and A. Bousseksou, *Chem. Phys. Lett.*, 2010, **499**, 94-99.
8. S. Pillet, E. Bendeif, S. Bonnet, H. J. Shepherd and P. Guionneau, *Phys. Rev. B*, 2012, **86**, 064106.
9. H. J. Shepherd, S. Bonnet, P. Guionneau, S. Bedoui, G. Garbarino, W. Nicolazzi, A. Bousseksou and G. Molnár, *Phys. Rev. B*, 2011, **84**, 144107.
10. S. Bonnet, G. Molnár, J. S. Costa, M. A. Siegler, A. L. Spek, A. Bousseksou, W. T. Fu, P. Gamez and J. Reedijk, *Chem. Mat.*, 2009, **21**, 1123-1136.
11. Z. Arcís-Castillo, S. Zheng, M. A. Siegler, O. Roubeau, S. Bedoui and S. Bonnet, *Chem.-Eur. J.*, 2011, **17**, 14826-14836.
12. P. Zhou, Y.-G. Zhao, Y. Bai, K.-L. Pang and C. He, *Inorg. Chim. Acta*, 2007, **360**, 3965-3970.
13. A. Hauser, *Top. Curr. Chem.*, 2004, **233**, 49-58.
14. J. M. Holland, J. A. McAllister, C. A. Kilner, M. Thornton-Pett, A. J. Bridgeman and M. A. Halcrow, *J. Chem. Soc. Dalton Trans.*, 2002, 548-554.
15. M. L. Scudder, D. C. Craig and H. A. Goodwin, *CrystEngComm*, 2005, **7**, 642-649.
16. J. McMurtrie and I. Dance, *CrystEngComm*, 2005, **7**, 216-229.
17. T. J. Mooibroek, P. Gamez and J. Reedijk, *CrystEngComm*, 2008, **10**, 1501-1515.
18. T. J. Mooibroek, C. A. Black, P. Gamez and J. Reedijk, *Cryst. Growth Des.*, 2008, **8**, 1082-1093.
19. O. Kahn, *Molecular Magnetism, Wiley VCH*, 1993.
20. M. A. Halcrow, *Chem. Soc. Rev.*, 2008, **37**, 278-289.
21. M. A. Halcrow, *Chem. Soc. Rev.*, 2011, **40**, 4119-4142.
22. *Unpublished Work.*